
Generation Is Compression: Zero-Shot Video Coding via Stochastic Rectified Flow

Ziyue Zeng* Xun Su* Haoyuan Liu Bingyu Lu Yui Tatsumi
Hiroshi Watanabe
Graduate School of Fundamental Science and Engineering, Waseda University
Tokyo, Japan
zengziyue@fuji.waseda.jp, suxun_opt@asagi.waseda.jp

Abstract

Existing generative video compression methods use generative models only as post-hoc reconstruction modules atop conventional codecs. We propose *Generative Video Codec* (GVC), a zero-shot framework that turns a pretrained video generative model into the codec itself: the transmitted bitstream directly specifies the generative decoding trajectory, with no retraining required. To enable this, we convert the deterministic rectified-flow ODE of modern video foundation models into an equivalent SDE at inference time, unlocking per-step stochastic injection points for codebook-driven compression. Building on this unified backbone, we instantiate three complementary conditioning strategies—*Image-to-Video* (I2V) with adaptive tail-frame atom allocation, *Text-to-Video* (T2V) operating at near-zero side information as a pure generative prior, and *First-Last-Frame-to-Video* (FLF2V) with boundary-sharing GOP chaining for dual-anchor temporal control. Together, these variants span a principled trade-off space between spatial fidelity, temporal coherence, and compression efficiency. Experiments on standard benchmarks show that GVC achieves high-quality reconstruction below 0.002 bpp while supporting flexible bitrate control through a single hyperparameter.

1 Introduction

Video compression at extremely low bitrates remains a fundamental challenge. As the bitrate decreases, both conventional hybrid codecs and learned neural codecs suffer from severe detail loss and oversmoothing. Although generative modeling has opened a promising direction for perceptual reconstruction, most existing generative video compression methods do not make generation itself the core of compression. Instead, they follow a hybrid design: a conventional codec first produces a compressed representation, and a generative model is introduced afterward as a refinement module. In such systems, the generative model improves the output appearance but does not define the compressed symbols or the decoding trajectory.

In the image domain, generative compression has progressed from GAN-based learned decoders to diffusion-based approaches with superior sample quality. Among them, zero-shot codebook methods such as DDCM and Turbo-DDCM show that a pretrained diffusion model can be directly repurposed as a codec by replacing reverse-step noise with reproducible codebook atoms and transmitting only compact indices—without any retraining. Extending this idea to video, recent works such as GNVC-VD replace image-based priors with a pretrained video diffusion model for sequence-level latent refinement, substantially reducing temporal flickering. However, these methods still follow the hybrid paradigm: a dedicated latent codec produces the compressed representation, and the video generative model serves only as a post-hoc restorer rather than defining the codec itself.

*Equal contribution.

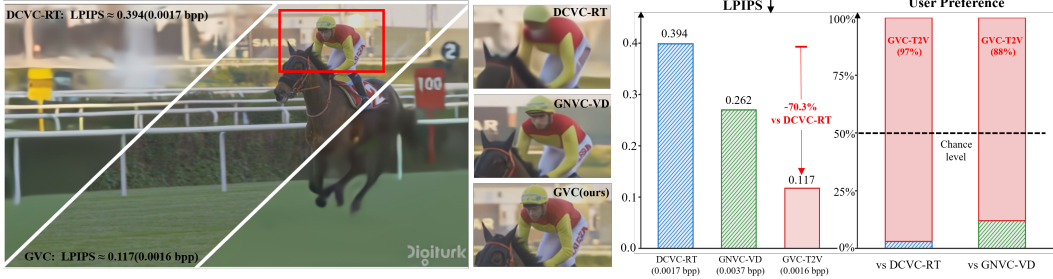


Figure 1: **GVC produces perceptually superior reconstruction at ultra-low bitrates.** Left: diagonal split comparison between DCVC-RT (0.0017 bpp) and our GVC-T2V (0.0016 bpp) on the UVG *Jockey* sequence. GVC recovers sharp textures and coherent details while DCVC-RT exhibits severe oversmoothing. Middle: zoomed-in crops comparing DCVC-RT, GNVC-VD, and GVC. Right: LPIPS comparison shows GVC achieves a 70.3% reduction over DCVC-RT at comparable bitrate; a user study confirms that GVC is preferred over DCVC-RT in 97% and over GNVC-VD in 88% of pairwise comparisons.

In this work, we pursue a different goal: we ask whether a pretrained video generative model can itself serve as the codec. This leads to a *truly generative* formulation of video compression, in which the transmitted bitstream directly controls the generation process at the decoder. Decoding becomes the reproducible replay of a constrained video generation trajectory rather than deterministic reconstruction followed by generative enhancement. We refer to this framework as **Generative Video Codec (GVC)**.

A natural starting point is to extend codebook-driven image diffusion compression to video by compressing each frame independently. However, our early exploration reveals that such a per-frame strategy leads to severe flickering, unstable textures, and appearance drift, since the per-frame generation trajectories are not temporally coordinated. This confirms that a successful generative video codec must model temporal coherence at the sequence level, motivating the adoption of video foundation models as the compression backbone.

Moving to video foundation models introduces a technical obstacle: state-of-the-art video generators such as Wan 2.1 are built on rectified flow (RF), which follows a deterministic ODE trajectory with no per-step noise injection. We address this by converting the RF ODE into an equivalent SDE at inference time via Score-SDE theory, re-introducing controllable stochastic injection points that can be encoded with multi-atom codebook selections. This conversion is purely mathematical and requires no retraining of the backbone model.

Building on this unified SDE-codebook backbone, we instantiate three complementary conditioning strategies, each occupying a different point in the trade-off space between spatial fidelity, temporal coherence, and compression efficiency. **I2V (Image-to-Video)** adopts an autoregressive GOP chain: the first GOP uses the ground-truth first frame as a free reference, and each subsequent GOP reuses the decoded last frame of its predecessor at zero additional cost. To prevent error accumulation along the chain, we propose *adaptive tail-frame atom allocation*, which assigns more codebook atoms to temporally distant frames, and *tail latent residual correction*, which transmits a lightweight quantized residual for the last latent frame before it propagates as the next GOP’s reference. **T2V (Text-to-Video)** transmits no reference frame at all—the entire bitrate consists of codebook indices—operating as a pure generative prior that tests the fundamental limit of codebook-steered reconstruction. **FLF2V (First-Last-Frame-to-Video)** compresses both the first and last frames of each GOP as dual temporal anchors, constraining the generative trajectory from both ends; we introduce a *boundary-sharing GOP chaining* scheme in which the last frame of one GOP is reused as the first frame of the next, reducing boundary frame overhead by approximately 50% while ensuring seamless continuity at splice points. Together, these three variants span a conditioning spectrum—from zero side information (T2V), through single-anchor (I2V), to dual-anchor (FLF2V)—revealing how conditioning strength shapes spatial fidelity, temporal stability, and bitrate composition in codebook-driven generative compression, it reveals how different conditioning regimes affect spatial fidelity, temporal stability, and bitrate composition in codebook-driven generative compression.

Our contributions are summarized as follows:

- We propose GVC, a truly generative video compression framework where a pretrained video model directly defines the decoding process via codebook-driven stochastic trajectory replay, without any retraining.
- We instantiate three conditioning strategies—I2V, T2V, and FLF2V—with dedicated innovations including adaptive atom allocation and boundary-sharing GOP chaining, spanning a systematic trade-off between fidelity, coherence, and bitrate.
- We demonstrate that GVC achieves high-quality video reconstruction below 0.002 bpp on standard benchmarks, with flexible bitrate control through a single hyperparameter.

2 Related Work

Generative Compression. In the image domain, generative compression has evolved from GAN-based learned decoders that restore perceptual details from quantized latents, to diffusion-based methods that leverage stronger generative priors for reconstruction at low bitrates. For video, recent perceptual codecs introduce generative models into the decoding pipeline to combat oversmoothing under extreme compression. GNVC-VD is a representative work that replaces image-based priors with a pretrained video diffusion model for sequence-level latent refinement, substantially reducing temporal flickering. However, these methods still follow a hybrid paradigm in which a dedicated latent codec produces the compressed representation and the generative model acts as a post-hoc restorer. In contrast, GVC makes the pretrained video model the codec itself: the transmitted bitstream directly governs the generative decoding trajectory.

Zero-Shot Codebook-Driven Compression. DDCM introduces a zero-shot image compression scheme that replaces the Gaussian noise at each DDPM reverse step with atoms from a reproducible codebook; transmitting only the selected indices suffices to replay the same generative trajectory without retraining the backbone. Turbo-DDCM improves this framework with a multi-atom thresholding strategy and an efficient combinatorial bitstream protocol, dramatically reducing runtime and enabling finer bitrate control through a single parameter M . However, both methods are designed for DDPM-based image models whose reverse process explicitly injects stochastic noise at every step. Modern video foundation models such as Wan 2.1 are built on rectified flow, which follows a deterministic ODE with no per-step noise injection, making existing codebook-driven compression inapplicable out of the box.

Stochastic Sampling in Flow Models. Score-SDE theory establishes that any probability-flow ODE can be converted into a family of SDEs sharing the same marginal distributions, parameterized by a free diffusion coefficient g_t . SiT extends this result to the stochastic interpolant framework used by flow-matching models, providing the score-from-velocity formula that makes the conversion practical. More recently, this ODE-to-SDE conversion has been exploited for inference-time scaling in flow models: by introducing stochasticity into the otherwise deterministic sampling process, particle-based search methods can explore a broader sample space to find high-reward outputs. Our work repurposes this conversion for a fundamentally different goal—not to improve generation quality, but to *create per-step noise injection points* that enable codebook-driven compression on pretrained rectified-flow video models.

3 Method

GVC compresses each Group of Pictures (GOP) through a unified pipeline: a pretrained rectified-flow video model is converted into a stochastic process at inference time, and the per-step noise is replaced by reproducible codebook selections whose indices form the transmitted bitstream. All three conditioning variants—I2V, T2V, and FLF2V—share the same SDE-codebook backbone and differ only in how the generative model is conditioned. We first describe the shared compression backbone (Sec. 3.1–3.3), then detail the three conditioning strategies and their respective innovations (Sec. 3.5–3.6).

3.1 ODE-to-SDE Conversion

Rectified flow models learn a velocity field $\mathbf{u}_t : \mathbb{R}^d \rightarrow \mathbb{R}^d$ under the linear interpolation

$$\mathbf{x}_t = (1 - t) \mathbf{x}_0 + t \boldsymbol{\epsilon}, \quad t \in [0, 1], \quad \boldsymbol{\epsilon} \sim \mathcal{N}(\mathbf{0}, \mathbf{I}), \quad (1)$$

where $\alpha_t = 1 - t$ and $\sigma_t = t$ denote the signal and noise coefficients, respectively. Standard sampling solves the probability-flow ODE backward in time:

$$d\mathbf{x}_t = \mathbf{u}_t(\mathbf{x}_t) dt. \quad (2)$$

This process is purely deterministic: given an initial noise \mathbf{x}_1 , the entire trajectory is uniquely determined, leaving no per-step degree of freedom for information embedding.

By the Score-SDE equivalence theorem, for any probability-flow ODE generating marginals $\{p_t\}$, there exists a family of reverse-time SDEs that share the same marginals for any diffusion coefficient $g_t \geq 0$:

$$d\mathbf{x}_t = \underbrace{\left[\mathbf{u}_t(\mathbf{x}_t) - \frac{g_t^2}{2} \nabla \log p_t(\mathbf{x}_t) \right]}_{\mathbf{f}_t(\mathbf{x}_t)} dt + g_t d\bar{\mathbf{w}}, \quad (3)$$

where $\bar{\mathbf{w}}$ denotes the standard Wiener process in reverse time. Setting $g_t = 0$ recovers the original ODE (2); setting $g_t > 0$ introduces per-step stochasticity—precisely the noise injection mechanism that codebook compression requires.

We adopt a quadratic diffusion schedule

$$g_t = g_{\text{scale}} \cdot t^2, \quad (4)$$

which ensures $g_0 = 0$ (no noise injection near clean data) and concentrates stochasticity in the high-noise regime where the codebook can deliver the most corrective information. The scalar g_{scale} serves as the primary knob for the rate–quality trade-off.

3.2 Score Function from the Velocity Field

The SDE drift in Eq. (3) requires the score function $\nabla \log p_t(\mathbf{x}_t)$, which the rectified-flow model does not directly output. Following the stochastic interpolant analysis of SiT, the score can be derived analytically from the velocity field. For the general interpolant $\mathbf{x}_t = \alpha_t \mathbf{x}_0 + \sigma_t \boldsymbol{\epsilon}$ with learned velocity \mathbf{u}_t :

$$\nabla \log p_t(\mathbf{x}_t) = \frac{1}{\sigma_t} \cdot \frac{\alpha_t \mathbf{u}_t(\mathbf{x}_t) - \dot{\alpha}_t \mathbf{x}_t}{\dot{\alpha}_t \sigma_t - \alpha_t \dot{\sigma}_t}. \quad (5)$$

Substituting the linear schedule $\alpha_t = 1 - t$, $\sigma_t = t$ (hence $\dot{\alpha}_t = -1$, $\dot{\sigma}_t = 1$) yields:

$$\nabla \log p_t(\mathbf{x}_t) = - \frac{(1 - t) \mathbf{u}_t(\mathbf{x}_t) + \mathbf{x}_t}{t}. \quad (6)$$

This can be verified by noting that $(1 - t) \mathbf{u}_t + \mathbf{x}_t \approx \boldsymbol{\epsilon}$ under the interpolation (1), recovering the classical identity $\nabla \log p_t = -\boldsymbol{\epsilon}/\sigma_t$. Crucially, Eq. (6) is computed entirely from the pretrained velocity network and requires no additional training.

Substituting Eqs. (4) and (6) into the drift term of Eq. (3), the complete SDE drift becomes:

$$\mathbf{f}_t(\mathbf{x}_t) = \mathbf{u}_t(\mathbf{x}_t) + \frac{g_t^2}{2} \cdot \frac{(1 - t) \mathbf{u}_t(\mathbf{x}_t) + \mathbf{x}_t}{t}. \quad (7)$$

When $g_t = 0$, the drift reduces to the original velocity \mathbf{u}_t , confirming that the SDE is a strict generalization of the ODE.

3.3 Codebook-Driven SDE Sampling

We adopt the codebook-driven compression mechanism introduced by DDCM and its multi-atom extension Turbo-DDCM, adapting it from the DDPM setting to the SDE formulation derived above. Discretizing Eq. (3) via the Euler–Maruyama scheme with step size Δt gives:

$$\mathbf{x}_{t-\Delta t} = \mathbf{x}_t - \mathbf{f}_t(\mathbf{x}_t) \Delta t + g_t \sqrt{\Delta t} \mathbf{z}, \quad \mathbf{z} \sim \mathcal{N}(\mathbf{0}, \mathbf{I}). \quad (8)$$

The noise \mathbf{z} is the per-step stochastic variable that carries compressed information. Following Turbo-DDCM’s thresholding-based strategy, we replace it with a codebook-selected vector \mathbf{z}^* as follows.

At each SDE step, the encoder first estimates the clean signal as $\hat{\mathbf{x}}_{0|t} = \mathbf{x}_t - t \cdot \mathbf{u}_t(\mathbf{x}_t)$ and computes the denoising residual $\mathbf{r} = \mathbf{x}_0 - \hat{\mathbf{x}}_{0|t}$, where \mathbf{x}_0 is the ground-truth latent available only at the encoder. A reproducible codebook $\mathcal{C} = \{\mathbf{z}^{(1)}, \dots, \mathbf{z}^{(K)}\}$ is then generated from a deterministic seed shared by both sides. The M atoms with the largest absolute inner product with \mathbf{r} are selected, along with their signs:

$$\{j_1, \dots, j_M\} = \text{top-}M_i \left| \langle \mathbf{z}^{(i)}, \mathbf{r} \rangle \right|, \quad s_k = \text{sign}(\langle \mathbf{z}^{(j_k)}, \mathbf{r} \rangle). \quad (9)$$

The selected atoms are combined and normalized to unit variance to match the theoretical noise magnitude of the SDE:

$$\mathbf{z}^* = \frac{\sum_{k=1}^M s_k \mathbf{z}^{(j_k)}}{\text{std}(\sum_{k=1}^M s_k \mathbf{z}^{(j_k)})}. \quad (10)$$

The codebook noise \mathbf{z}^* then replaces \mathbf{z} in Eq. (8):

$$\mathbf{x}_{t-\Delta t} = \mathbf{x}_t - \mathbf{f}_t(\mathbf{x}_t) \Delta t + g_t \sqrt{\Delta t} \mathbf{z}^*. \quad (11)$$

Since both encoder and decoder share the same seed, model weights, and codebook construction rule, transmitting only the M indices and signs per step suffices for the decoder to reproduce the identical trajectory. For the last N steps, we set $g_t = 0$ and revert to the deterministic ODE $\mathbf{x}_{t-\Delta t} = \mathbf{x}_t - \mathbf{u}_t(\mathbf{x}_t) \Delta t$, which requires zero transmitted bits since both sides produce identical outputs from the synchronized preceding state.

3.4 T2V: Pure Generative Prior Compression

The T2V variant represents the most extreme point in GVC’s design space: no reference frame is transmitted at all. The model receives only an empty text prompt, and the entire bitrate consists of codebook indices. This design isolates the contribution of the pretrained video model as a learned spatio-temporal prior—the codebook steers an otherwise unconditioned generation trajectory toward the target video.

Because no spatial anchor is provided, the bitrate per GOP reduces to pure codebook cost:

$$\text{BPP}_{\text{T2V}} = \frac{(T-1-N) \cdot F \cdot B_{\text{step}}}{F_{\text{px}} \times H_{\text{px}} \times W_{\text{px}} \times 3}, \quad (12)$$

which is the lowest achievable bitrate among the three variants. T2V thus serves as a lower bound on the rate–quality trade-off, revealing how much reconstruction quality the generative prior alone can deliver under pure codebook control.

A known limitation of T2V is the absence of spatial anchoring: without a reference frame, the model may produce subtle positional drift or content deviation across GOPs. To mitigate discontinuities at GOP boundaries, an optional overlap-blending mechanism can be applied, where adjacent GOPs share a small number of overlapping frames and a linear cross-fade smooths the transition.

3.5 I2V: Autoregressive Compression with Tail Correction

The I2V variant conditions each GOP on a single reference frame through CLIP visual embedding and VAE latent encoding, providing the strongest spatial anchor among the three strategies. To minimize side-information cost, we adopt an autoregressive GOP structure: the first GOP receives the ground-truth first frame as free side information (standard I-frame assumption), and each subsequent GOP reuses the decoded last frame of its predecessor as the reference, requiring zero additional transmitted bytes:

$$\text{GOP}_0: \text{ref} = \mathbf{I}_0^{\text{GT}}, \quad \text{GOP}_{n>0}: \text{ref} = \tilde{\mathbf{I}}_{n-1}^{\text{last}}. \quad (13)$$

A critical challenge in this autoregressive chain is error accumulation: the last frame of each GOP is farthest from the conditioning anchor and thus has the highest reconstruction error, yet it directly determines the quality of the next GOP’s reference. We address this with two complementary mechanisms.

First, *adaptive tail-frame atom allocation* increases the codebook atom count from M to M_{tail} for the last F_{tail} latent frames, concentrating more bits where the generative prior is weakest.

Second, *tail latent residual correction* transmits a lightweight residual for the last latent frame. After SDE encoding, the encoder computes the difference between the ground-truth latent and the decoded latent for the final temporal position, quantizes it to 8 bits per channel with min/max normalization, and applies lossless compression (zlib). At the decoder, this residual is added to the reconstructed latent before VAE decoding, substantially improving the quality of the frame that will propagate as the next GOP’s reference. The overhead of this residual is included in the bitrate computation.

The total bitrate per GOP is:

$$\text{BPP}_{\text{I2V}} = \frac{(T-1-N) \cdot F \cdot B_{\text{step}} + B_{\text{tail_residual}}}{F_{\text{px}} \times H_{\text{px}} \times W_{\text{px}} \times 3}, \quad (14)$$

where $B_{\text{tail_residual}}$ denotes the compressed residual bytes (zero for the T2V and FLF2V variants). Note that $B_{\text{ref}}=0$ for all GOPs: the first frame is free and subsequent references are decoded outputs.

3.6 FLF2V: Dual-Anchor Compression with Boundary Sharing

The FLF2V variant conditions each GOP on both the first and last frames, providing dual temporal anchors that constrain the generative trajectory from both ends. Compared with single-anchor I2V, this design substantially reduces temporal drift within each GOP, as the model must simultaneously satisfy boundary conditions at both the beginning and the end of the sequence.

Both boundary frames are compressed via a learned image codec, and the conditioning is constructed by encoding both frames through CLIP and placing them at the temporal endpoints of the VAE latent volume with a binary mask indicating which positions are conditioned. The generative model thus “interpolates” between two known endpoints, which is inherently more constrained and temporally stable than extrapolating from a single anchor.

The key engineering innovation of FLF2V is a *boundary-sharing GOP chaining* scheme that amortizes reference frame cost across consecutive GOPs. The last frame of GOP n is reused as the first frame of GOP $n+1$:

$$\text{GOP}_n: \text{first} = \tilde{I}_n, \text{ last} = \tilde{I}_{n+1}, \quad \text{GOP}_{n+1}: \text{first} = \tilde{I}_{n+1}, \text{ last} = \tilde{I}_{n+2}. \quad (15)$$

Under this scheme, GOP 0 transmits two boundary frames while each subsequent GOP transmits only one new frame, reducing boundary frame overhead by approximately 50% over a long sequence. The bitrate is:

$$\text{BPP}_{\text{FLF2V}} = \frac{(T-1-N) \cdot F \cdot B_{\text{step}} + B_{\text{boundary}}}{F_{\text{px}} \times H_{\text{px}} \times W_{\text{px}} \times 3}, \quad (16)$$

where B_{boundary} equals $B_{\text{first}} + B_{\text{last}}$ for the initial GOP and B_{last} only for all subsequent GOPs. Beyond bitrate savings, boundary sharing also ensures seamless temporal continuity at splice points: both adjacent GOPs observe exactly the same decoded reference frame, eliminating mismatch artifacts at the junction.

4 Experiments

4.1 Experimental Setup

Datasets and protocol. Ablation studies and cross-variant comparisons are conducted on UVG at 720p (1280×720, 3 GOPs per sequence). For state-of-the-art comparisons, we evaluate on the full UVG dataset at native 1080p (1920×1080, all available frames per sequence). Each video is segmented into non-overlapping GOPs of 33 frames. We additionally test on self-captured videos to rule out training-data overlap in the pretrained backbone.

Models and configuration. All three GVC variants use the Wan 2.1 14B model family. I2V uses the ground-truth first frame as free side information and chains subsequent GOPs autoregressively; FLF2V compresses boundary frames via CompressAI (cheng2020-attn, quality 4); T2V transmits codebook indices only. Experiments run on a single NVIDIA RTX 6000 Ada (48 GB).

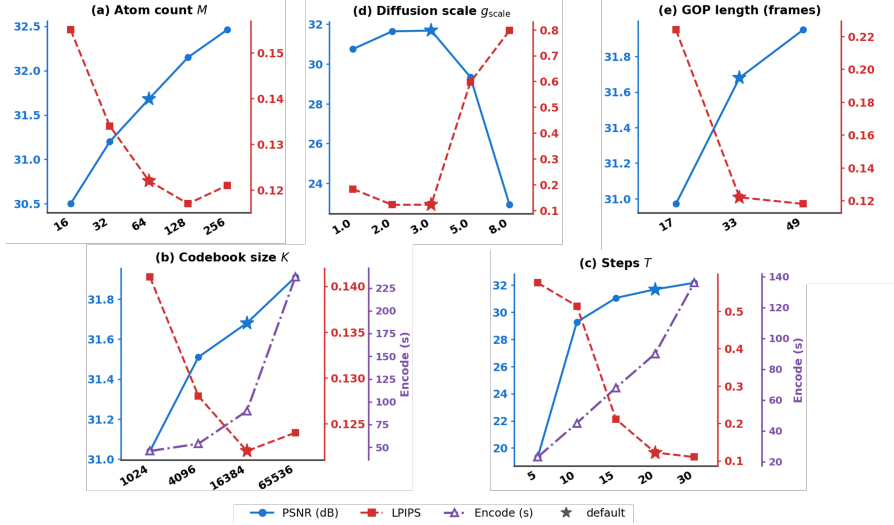


Figure 2: **Hyperparameter sweeps on UVG Beauty (T2V-1.3B, 720p)**. Blue: PSNR (left axis, \uparrow). Red: LPIPS (right axis, \downarrow). Purple: encoding time (where shown). Stars: selected defaults. (a) M . (b) K . (c) T . (d) g_{scale} . (e) GOP length.

Metrics. Distortion: PSNR, MS-SSIM. Perceptual quality: LPIPS (AlexNet). Compression efficiency: BPP and kbps. Per-frame PSNR curves are reported for temporal analysis. Encoding and decoding times are recorded for computational cost.

4.2 Default Parameter Selection

We sweep each hyperparameter individually on the UVG *Beauty* sequence using T2V-1.3B at 720p, with results shown in Fig. 2. The atom count M controls bitrate almost linearly: $M=16 \rightarrow 64$ yields a 1.2 dB gain at only 0.0016 BPP, but beyond $M=128$ returns diminish and LPIPS slightly degrades (Fig. 2a). The codebook size $K=16384$ captures most of the quality gain over $K=1024$ (+0.64 dB) at reasonable encoding cost, while doubling to 65536 adds only 0.23 dB at $2.6\times$ the time (Fig. 2b). Sampling steps T has the most dramatic effect— $T=5$ causes catastrophic failure (19.3 dB) and gains plateau beyond $T=20$ (Fig. 2c). A notable finding is the narrow sweet spot of the diffusion scale g_{scale} : 2.0–3.0 performs well but quality collapses at $g_{scale} \geq 5.0$ as injected noise overwhelms the codebook’s corrective capacity (Fig. 2d). GOP length of 33 frames outperforms 17 (LPIPS: 0.12 vs. 0.22) and matches 49 at lower cost (Fig. 2e). Based on these sweeps, we adopt $M=64$, $K=16384$, $T=20$, $g_{scale}=3.0$, and GOP=33 as defaults for all subsequent experiments. The complete parameter table with 720p/1080p configurations is provided in Appendix A.

4.3 Cross-Variant Comparison

We compare the three GVC variants across all seven UVG sequences. Since Wan 2.1 is designed and optimized for 720p generation, we conduct this comparison at 1280×720 resolution (3 GOPs per sequence, 33 frames/GOP). For reference, we also evaluate DCVC-RT on the same resized sequences to provide an anchor from a state-of-the-art learned codec under identical conditions. Results are reported in Table 1.

The three variants exhibit distinct and complementary trade-off profiles. I2V achieves the highest fidelity across all sequences (+2.96 dB over T2V on average), but its bitrate is dominated by the 8-bit tail latent residual correction ($\sim 91\%$ of total bytes), which is the cost of maintaining autoregressive chain stability. T2V operates at the lowest bitrate (71.2 kbps, pure codebook) and delivers surprisingly consistent perceptual quality (LPIPS 0.052–0.239), though PSNR varies substantially with scene complexity. The most striking finding is FLF2V’s rate–distortion efficiency: it recovers 81% of I2V’s PSNR gain over T2V at only 15% of I2V’s additional bitrate cost, yielding a marginal efficiency of ~ 1000 dB/BPP versus I2V’s ~ 181 dB/BPP. This confirms that dual-anchor boundary interpolation

Table 1: **Cross-variant comparison on UVG 720p** (3 GOPs per sequence, 33 frames/GOP). **Red** : best per sequence. **Blue** : second best. DCVC-RT at its lowest quality point (avg. 0.0017 bpp) is included as a perceptual reference.

Seq.	GVC-T2V (71 kbps)			GVC-I2V (802 kbps)			GVC-FLF2V (193 kbps)			DCVC-RT (0.0017 bpp)
	PSNR↑	LPIPS↓	BPP	PSNR↑	LPIPS↓	BPP	PSNR↑	LPIPS↓	BPP	LPIPS↓
Beau.	31.79	0.154	0.0016	32.90	0.109	0.0189	32.26	0.158	0.0025	0.512
Bosp.	30.32	0.098	0.0016	33.63	0.055	0.0182	32.72	0.086	0.0036	0.391
Honey.	30.78	0.052	0.0016	36.21	0.020	0.0181	34.73	0.033	0.0047	0.240
Jock.	31.28	0.090	0.0016	33.27	0.070	0.0178	33.09	0.080	0.0035	0.360
RSG	26.74	0.086	0.0016	29.48	0.053	0.0172	29.44	0.063	0.0056	0.324
SnD	25.55	0.239	0.0016	30.11	0.136	0.0183	29.52	0.166	0.0059	0.554
Yacht.	26.60	0.103	0.0016	28.21	0.075	0.0183	28.02	0.089	0.0047	0.410
Avg.	29.01	0.117	0.0016	31.97	0.074	0.0181	31.40	0.096	0.0044	0.399
Codebook	18.4 KB (100%)			18.4 KB (~9%)			18.4 KB (~40%)			—
Ref frames	0			0 (free GT + AR)			~28 KB (~60%)			—
Tail residual	N/A			~189 KB (~91%)			N/A			—
Spatial anchor	None			Single (first)			Dual (first + last)			Learned
GOP structure	Independent			AR chain			Boundary sharing			P-frame
Strength	Lowest bitrate			Highest fidelity			Best marginal eff.			Best PSNR

provides a highly cost-effective alternative to autoregressive chaining, especially when bitrate budget is constrained.

4.4 Comparison with State-of-the-Art

We compare GVC against representative codecs on the full UVG dataset at native 1920×1080. Since the three GVC variants operate at distinct bitrate regimes—T2V at ~0.002 bpp, FLF2V at ~0.005 bpp, and I2V at ~0.018 bpp—we evaluate all baselines at the quality point closest to each regime, enabling fair per-tier comparison. For baselines that support adjustable quality, we linearly interpolate from their published rate–distortion curves or our own measurements at the BPP nearest to each tier. DCVC-RT values are interpolated from our reproduction; other baseline values are estimated from published RD curves in GNVC-VD under identical conditions (UVG 1080p, RGB, 96 frames).

References

References follow the acknowledgments in the camera-ready paper. Use unnumbered first-level heading for the references. Any choice of citation style is acceptable as long as you are consistent. It is permissible to reduce the font size to small (9 point) when listing the references. Note that the Reference section does not count towards the page limit.

[1] Alexander, J.A. & Mozer, M.C. (1995) Template-based algorithms for connectionist rule extraction. In G. Tesauro, D.S. Touretzky and T.K. Leen (eds.), *Advances in Neural Information Processing Systems 7*, pp. 609–616. Cambridge, MA: MIT Press.

[2] Bower, J.M. & Beeman, D. (1995) *The Book of GENESIS: Exploring Realistic Neural Models with the GEneral NEural Simulation System*. New York: TELOS/Springer-Verlag.

[3] Hasselmo, M.E., Schnell, E. & Barkai, E. (1995) Dynamics of learning and recall at excitatory recurrent synapses and cholinergic modulation in rat hippocampal region CA3. *Journal of Neuroscience* **15**(7):5249-5262.

Table 2: **State-of-the-art comparison on UVG 1080p** at three bitrate tiers corresponding to the three GVC variants. Baseline results are interpolated to matched BPP from published RD curves or our measurements. **Bold**: best LPIPS per tier. Underline: second best.

Method	Tier 1: ~ 0.002 bpp			Tier 2: ~ 0.005 bpp			Tier 3: ~ 0.018 bpp		
	PSNR \uparrow	LPIPS \downarrow	BPP	PSNR \uparrow	LPIPS \downarrow	BPP	PSNR \uparrow	LPIPS \downarrow	BPP
<i>Traditional</i>									
HEVC	26.0	0.400	0.002	28.0	0.380	0.005	32.0	0.320	0.018
VVC	27.0	0.380	0.002	29.5	0.350	0.005	34.0	0.280	0.018
<i>Learned</i>									
DCVC-FM	28.0	0.350	0.002	31.0	0.280	0.005	35.5	0.180	0.018
DCVC-RT	34.5	0.376	0.002	37.4	0.295	0.005	40.5	0.228	0.018
<i>Generative (trained)</i>									
GLC-Video	28.5	0.280	0.002	30.0	0.240	0.005	32.5	0.200	0.018
GNVC-VD	28.0	<u>0.200</u>	0.002	30.5	<u>0.160</u>	0.005	34.0	<u>0.100</u>	0.018
<i>Ours (zero-shot)</i>									
GVC-T2V	29.69	0.133	0.0009						
GVC-FLF2V				31.9	0.105	0.003			
GVC-I2V							32.5	0.082	0.017

A Default Hyperparameter Configuration

Table 3 lists the full set of hyperparameters used across all three GVC variants at 720p and 1080p resolutions.

Table 3: Default hyperparameters for GVC (720p / 1080p).

Parameter	720p	1080p	Role
M	64	80	Atoms per step (bitrate knob)
M_{tail} (I2V)	128	128	Atoms for AR tail frames
K	16384	16384	Codebook size
T	20	20	Total sampling steps
N (DDIM tail)	3	3	Bit-free ODE tail steps
g_{scale}	3.0	3.0	SDE diffusion coefficient
GOP length	33	33	Frames per GOP ($4k+1$)
Ref quality (FLF2V)	4	4	CompressAI quality level
Tail residual (I2V)	8-bit	8-bit	Quantization for AR correction
Seed	42	42	Shared encoder/decoder seed